Life fingerprints of nuclear reactions in the body of animals

Jun Zeng[1,2], Qi-yin Sun[1], Tao Sun[2], Ji-hui Su[2], Ji-hui Han[2], Quan-shi Zhang[2], Wen-hui Xie[3], Ci-yi Liu[3], and Xiao-jia Cai[3]

1 Medical R&D center, Top Grade & Kang-Ming Ltd, Beijing, PRC
2 Wu-xi Yi-ren Cancer Hospital, Jiangsu Wuxi (Huishan) Life Science Technology Park, Wu-xi, PRC
3 Shanghai Chest Hospital, Shanghai Jiao-tong University, Huai-hai West Road, Shanghai, PRC

Correspondence and requests for materials to: Jun Zeng (jzeng2002@sohu.com)

Abstract

Nuclear reactions are a very important natural phenomenon in the universe. On the earth, cosmic rays constantly cause nuclear reactions. High energy beams created by medical devices also induce nuclear reactions in the human body. The biological role of these nuclear reactions is unknown. Here we show that the in vivo biological systems are exquisite and sophisticated by nature in influence on nuclear reactions and in resistance to radical damage in the body of live animals. In this study, photonuclear reactions in the body of live or dead animals were induced with 50-MeV irradiation. Tissue nuclear reactions were detected by positron emission tomography (PET) imaging of the induced β+ activity. We found the unique tissue "fingerprints" of β+ (the tremendous difference in β+ activities and tissue distribution patterns among the individuals) are imprinted in all live animals. Within any individual, the tissue "fingerprints" of ^{15}O and ^{11}C are also very different. When the animal dies, the tissue "fingerprints" are lost. The biochemical, rather than physical, mechanisms could play a critical role in the phenomenon of tissue "fingerprints". Radiolytic radical attack caused millions-fold increases in ^{15}O and ^{11}C activities via different biochemical mechanisms, i.e. radical-mediated hydroxylation and peroxidation respectively, and more importantly the bio-molecular functions (such as the chemical reactivity and the solvent accessibility to radicals). In practice biologically for example, radical attack can therefore be imaged in vivo in live animals and humans using PET for life science research, disease prevention, and personalized radiation therapy based on an

individual's bio-molecular response to ionizing radiation.

Nuclear reactions are a very important natural phenomenon in the universe. Cosmic rays constantly cause nuclear reactions on the earth. High-energy bremsstrahlung beams[1], proton beams[2], and heavy ion beams[2, 3] from medical facilities for cancer treatment also induce nuclear reactions in the human body. The biological role of these nuclear reactions is unknown. Like proton beams and heavy ion beams[2, 3], the activation of organ tissues by high-energy bremsstrahlung beams results primarily in ^{15}O and ^{11}C [1, 4, 5]. The process involves the conversion of normal ^{16}O and ^{12}C to ^{15}O and ^{11}C, respectively, by knocking out neutrons, the typical photonuclear reaction[4]. Thus, the nuclear reactions can be detected by positron emission tomography (PET) imaging of the induced β+ activity of ^{15}O and ^{11}C[1, 4, 5]. With the same irradiation factors, the relative ^{15}O and ^{11}C product yields are proportional to the normal ^{16}O and ^{12}C contents in the tissues[4], i.e., $^{16}O(\gamma,n)^{15}O$ and $^{12}C(\gamma,n)^{11}C$. Thus, the β+ emitters ^{15}O and ^{11}C in the tissue are proportional to the photon fluence and, approximately, to the absorbed dose[5]. Serendipitous findings of the animal tissue distributions of ^{15}O and ^{11}C activities were proven to be more complicated than is explained by basic physics. We found that biological, rather than physical, mechanisms could play the critical role in photonuclear reactions in the body of live animals.

Animals were selected randomly for irradiation studies. After simultaneously exposing the animals to 1.5 Gy of whole-body 50-MeV irradiation, the whole-body β+ activities and tissue distribution patterns of ^{15}O and ^{11}C were tremendously different among the individual live animals. However, animals with similar body weights maintained the same physiological conditions. This individual discrepancy in tissues is described here as the tissue "fingerprint". Each individual live animal's tissue "fingerprints" of ^{15}O and ^{11}C are unique. The tissue "fingerprints" are also very different between ^{15}O and ^{11}C for each individual. The biological phenomenon of

tissue "fingerprints" was observed in mice (Fig. 1A), rats (Fig. 1B) and rabbits (Figs. 1C, 2A and 2B). Local irradiation could also induce local tissue "fingerprints" of ^{15}O and ^{11}C in live rabbits (Fig. 1C).

More interestingly and unexpectedly, the rapid change in whole-body β+ activities and tissue distribution patterns of ^{15}O and ^{11}C were recorded by PET imaging before and up to 30 minutes after respiratory and cardiac arrest of animals. The tissue "fingerprints" faded away soon after death; the whole-body β+ activities and tissue distribution patterns became similar among animals (Fig. 2A-D), and for each individual animal, the distribution patterns became similar between ^{15}O and ^{11}C (Fig. 2A-D). An example of a tissue dynamically losing a ^{11}C "fingerprint" is shown in Fig. 2E. As the tissue activities changed after death, the dynamic decrease of the $^{15}O/^{11}C$-ratio was measured (Fig. 2F). Because the tissue "fingerprints" faded, the $^{15}O/^{11}C$-ratio changed from heterogeneous (Fig. 2G) to homogeneous (Fig. 2H) among different organs.

We found that the live animal tissue ^{15}O related to radical-mediated hydroxylation. 1,2-dibromoethane was used as a molecular model. The hydroxyl radical (OH·) oxidation mechanism of 1,2-dibromoethane involves OH· substitution reactions to form oxalyl dibromide [BrC(O)C(O)Br] and oxalic acid (HOOC-COOH)[6]. After exposing a liposome mixture of 1,2-dibromoethane and water (in this solution only water contained ^{16}O) to 5 Gy of 50-MeV irradiation, the radicals, which were generated by water radiolysis, triggered substitution reactions on 1,2-dibromoethane. An 8.5-fold increase in ^{15}O activity from hydroxyl and carbonyl products was released to the aqueous phase from the organic phase (Fig. 3A and 3B, Supplementary Fig.1). It has been extensively demonstrated by pulse-radiolysis experiments[7, 8] that a dose of about 5 Gy generates approximately 4.0 μM OH·. Using oxalic acid as the standard, we determined that the concentration of carbonyl products was 0.0163±0.0021 μmol/ml (n=6), which was about four-fold higher than that of OH· reported in previous studies (probably as a

result of the oxalyl bromides). The average ^{15}O activity was calculated as 107114.4±9152.7 cpm/μmol from the carbonyl products, and water control was measured as 0.004347±0.001219 cpm/μmol. Thus, the radical-mediated reactions increased ^{15}O activity by an average of 24,640,994±3,438,904-fold in the mixture of 1,2-dibromoethane and water. The average ^{11}C activity from the carbonyl products was only 3771.4±645.2 cpm/μmol, and the average increase was 249,760±14,857 times that of the 1,2-dibromoethane control, which was measured as 0.015132±0.003011 cpm/μmol.

Benzoic acid, which has low toxicity, was chosen to probe an in vivo radical-mediated hydroxylation as its fluorescent hydroxyl products accumulated in a rabbit liver. OH·-mediated hydroxylation can occurred on benzoic acid to form the corresponding 4-hydroxyl and 3,4-dihydroxyl derivatives[9]. The fluorescence intensity increases in proportion to the concentration of the hydroxyl derivative. Unlike benzoic acid, the hydroxyl derivatives are not the specific substrates for benzoyl-CoA ligase in liver[10]. Exposure to 5.5 Gy of 50-MeV irradiation resulted in local tissue "fingerprints" of ^{15}O and ^{11}C in individual live animals (Fig. 1C). An excellent correlation ($r=0.943231$, $n=29$) was found between ^{15}O activity and hydroxyl products of benzoic acid in the liver tissue (Fig. 3C). Both ^{11}C activity ($r=0.324333$, $n=29$) and dose delivery ($r=0.34053$, $n=29$) have a negligible relationship with the hydroxyl products (Fig. 3E and Supplementary Fig. 2A).

Here, we determined 8-OHdG as the biomarker to test the in vivo radical-mediated hydroxylation of a DNA element. It was determined that X-rays induce hydroxylation of a deoxyguanosine at the C-8 position by OH· to form an 8-hydroxydeoxyguanosine (8-OHdG)[11]. The DNA damage caused by 8-OHdG has been widely studied as a critical biomarker of oxidative stress and carcinogenesis. After whole-body exposure to 1.5 Gy of 50-MeV irradiation, tissue "fingerprints" of ^{15}O and ^{11}C were detected in each individual live mouse (Fig. 1A). After a

second high dose of 4.0 Gy/10-MeV irradiation, the levels of serum 8-OHdG ranged from 21.49 to 100.02 ng/L (52.32±20.97 ng/L) and correlated well with the whole-body ^{15}O activity (r=0.72623, n=64) (Fig. 3D). However, the levels of serum 8-OHdG were not correlated with the whole-body ^{11}C activity (r=-0.05325, n=64)(Fig. 3F).

The irradiation-induced dysfunction of proteins is based on the OH·-mediated modifications of the side chains of amino acids and peptide chain breaks. OH· exposure inhibits ATPase activity through a direct attack on the ATP binding site[12] and on the associative proteins[13]. After receiving 1.5 Gy of whole-body 50-MeV irradiation followed by a second dose of 6.0 Gy of 6-MeV irradiation, the ^{15}O and ^{11}C activities had an inverse correlation with the liver ATPase functions of ATP enzymolysis in live rats (Supplementary Fig.3). This indicates that tissue accumulation of ^{11}C activity may also be a result of the radical-mediated reactions instead of the hydroxylation.

We demonstrated that the live animal tissue ^{11}C related to radical-mediated peroxidation. At the initial stage of peroxidation, OH· can abstract a hydrogen atom from attacked molecules (e.g., ethanol and lipids), and in many cases, the final products are aldehydes[14, 15]. Using ethanol as a molecular model, exposure of an ethanol-water (in this solution only ethanol had ^{12}C) solution to 5.0 Gy of 50-MeV irradiation induced water radiolysis and triggered peroxidation reactions of ethanol, which caused a 30% increase ($p<0.00000001$) of ^{11}C activity (Fig. 4A, 4B). No significant change ($P>0.8$) in ^{15}O activity was detected after these reactions (Fig. 4A, 4B). The peroxidation reactions generated 0.0109±0.0014 μmol/ml (n=6) of carbonyl products, and the average ^{11}C activity from carbonyl products was calculated as 15562.4±2412.4 cpm/μmol. As a control, an exposure to ethanol gave an average ^{11}C activity of only 0.015768±0.002534 cpm/μmol. The peroxidation reactions of ethanol boosted the ^{11}C activity by an average of 986,961±88,126-fold.

Fluorescein sodium salt (FL) was used to probe in vivo the radical peroxidation. The reaction products of FL with

peroxyl radicals have been characterized, and the product pattern was consistent with a classic hydrogen atom transfer (HAT) reaction mechanism[16]. As the reaction progresses, FL is consumed, and fluorescence intensity decreases. As the prototypical organic anion, FL is stable in vivo due to mitochondrial storage[17]. The low toxicity of FL allows clinical injection for fluorescence angiography and diagnosis of diseases[18]. A strong correlation was shown between ^{11}C activity and FL intensity in the livers of live rabbits (r=-0.82144, n=36) (Fig. 4C). However, FL intensity was not well correlated with the delivery dose (r=-0.44131, n=36) (Supplementary Fig. 2B), and there was a poor correlation with ^{15}O activity (r=-0.21487, n=36) (Fig. 4E).

Malondialdehyde (MDA) was measured as a biomarker for lipid peroxidation. OH· reactions with lipids are typical HAT reactions during the first phase of lipid peroxidation. The secondary products are mainly aldehydes, and the major compound is MDA[19]. Irradiation-induced oxidative damage in a rat liver can elevate the level of MDA[20]. After whole-body irradiation with a single dose of 1.5 Gy/50-MeV, the tissue "fingerprints" of ^{15}O and ^{11}C for each of the live rats were as shown in Fig. 1B. After receiving a second high dose of 6.0 Gy/6-MeV irradiation, the levels of liver MDA correlated well with the liver ^{11}C activity (r=0.75239, n=54) (Fig. 4D). The level of liver MDA, however, was not correlated with the liver ^{15}O activity (r=0.08349, n=54) (Fig. 4F). Irradiation-induced dysfunction of liver ATPase correlated well with the accumulation of ^{11}C product (Supplementary Fig. 3).

Influence of hydrated electrons (eaq-) on β+ activities was tested with methanol. Oxidation of methanol with radicals involves both hydroxylation and HAT peroxidation to form formic acid and formaldehyde. In a 33% methanol-water solution (pH 4.5), irradiation with a single 5 Gy/50 MeV dose generated similar concentrations of hydrated formaldehyde and total carbonyls in oxygen-free, oxygenated, and e_{aq}- free (N_2O/O_2) conditions (see

Table 1). The carbonyl groups and the benzene rings of many compounds represent the principal trapping center for e_{aq}^- in oxygen-free solutions. OH· attack can further increase ^{11}C activity in e_{aq}^- free solutions due to the conversion of e_{aq}^- to OH· by N_2O/O_2, whereas an e_{aq}^- attack can further increase the ^{15}O activities in oxygen-free solutions (see Table 1).

Tissue "fingerprints" did not obviously follow the physical principle that nuclear reactions are completely independent of chemical reactions. A detailed mechanism of the physicochemical reactions is beyond the scope of this article, but these reactions, such as hydrogen atom transfer[21], electron transfer[21] and perhaps proton-coupled electron transfer[22], are worthy of future study. Logically, tissue accumulation of ^{15}O and ^{11}C activities may contribute to (1) the normal ^{16}O and ^{12}C contents, (2) the free radical attack (Figs. 3 and 4) and reaction conditions (Table 1), (3) the pool of antioxidants[23] (Supplementary Fig. 4), and (4) the bio-molecular functions[24]. Tissue "fingerprints" are obviously biological dependent because tissue "fingerprints" are related to biomarkers and protein function (Figs. 3 and 4 and Supplementary Fig. 4). And when life is lost, the tissue "fingerprints" are lost. The changes in the normal ^{16}O and ^{12}C contents and in the antioxidant contents are not expected in such short period of time. It seems that all reactive residues of molecules in tissues became accessible to radicals in an anaerobic condition (i.e., after respiratory and cardiac arrest; see Fig. 2C and 2D). Thus, the bio-molecular functions such as the chemical reactivity and the solvent accessibility to radicals[24, 25], may play a key role in the phenomenon of tissue "fingerprints". The scientific significance needs to be further elucidated.

Free radical-related damage and antioxidation is always one of the top concerns in the occurrence of disease (e.g., inflammation, cardiovascular disease, cancer, and aging-related disorders). In 1950s, Gerschman and Harman revealed that the toxic effects of oxygen were similar to the damage caused by X –ray irradiation[26, 27], and the second thought was that free radicals had major consequences to fundamental biological processes[28]. Decades later we understood further the free radical mediated mechanisms of disease by dysregulation of signal

transduction and/or by oxidative damage to cellular lipids, proteins, DNA, carbohydrates[29-31]. The major obstacle in free radical research is the lack of specific, sensitive, and noninvasive methods to analyze, in detail, radical attack in live animals, including human beings[32]. Therefore, the PET imaging of radical attack is a practical means to achieve this goal. Tissue "fingerprints" indicate that radical attack in vivo biological systems could be much more complicated than those described under in vitro conditions[21], and the in vivo biological systems are exquisite and sophisticated by nature (independent from the so called antioxidants) in resistance to radical damage and influence on nuclear reactions in the body of live animals.

Ionizing radiation is an important treatment modality in the management of cancers, and approximately 60% of cancer patients are treated with radiation therapy[33]. Our findings challenge the practice of radiotherapy in which, unlike ^{15}O and ^{11}C(Figs.3 and 4), the delivered does not correlate well with the bio-molecular damage by radiolytic oxidation (Supplementary Fig. 3). Tissue "fingerprints" bring to mind the inherent radiosensitivity. There is evidence to suggest that individual differences in inherent radiosensitivity do exist, so understanding their biological basis could significantly impact how clinical radiation oncology is practiced[33]. The development of a successful clinical assay to predict response to radiation therapy is a major clinical goal in radiation oncology. Radiolysis of water is the major mechanism of toxic effects, which can be traced back to radical-induced damage of DNA, proteins, or membrane lipids[34, 35]. The concept of personalized radiation therapy is therefore derived from the in vivo imaging of a radical attack in patients. After a low dose of exposure, the bio-molecular responses to ionizing radiation, in both the treatment target volume and surrounding normal tissues, can be detected by the PET/CT imaging of tissue "fingerprints". The clinical impact of this technology could result in better selection of patients for radiotherapy protocols, improve the assessment of individual response and prognosis, and lead to personalized radiation dose parameters.

Methods Summary

High-energy (50-MeV) bremsstrahlung beams, available from the MM50 Racetrack Microtron, were used to convert normal ^{16}O and ^{12}C to the positron emitters ^{15}O and ^{11}C. The total activity and ^{11}C ($T_{1/2}$=20.38 min) activity were separately recorded in the early phase and delayed phase of PET scanning. The ^{11}C activity was subtracted from the early total activity to obtain the ^{15}O activity ($T_{1/2}$=2.03 min). In the animal experiments, 1.5 Gy and 5.5 Gy of dose delivery were used for whole-body and local irradiation, respectively. Methanol, 1,2-dibromoethane, and ethanol were tested for radical-mediated hydroxylation and peroxidation. Irradiation of 5 Gy with 50 MeV started the radical reactions in a solution of ethanol (or methanol)-water (V:V=1:2) or in a liposome formation of 1,2-dibromoethane-water (V:V=1:1). Separate irradiations of 1,2-dibromoethane, methanol, ethanol and water were used for controls. The total carbonyl products were measured to calculate the ^{15}O and ^{11}C activities resulting from radical attack. For the analysis of $OH\cdot$ and e_{aq}- attack, N_2 (oxygen-free), O_2 (oxygenated) and N_2O (the e_{aq}- scavenger) were used. High performance liquid chromatography (HPLC) with a gamma detector was used to detect radio-products after radical attack. With the anatomic markers, both benzoic acid and fluorescein sodium salt (FL) were tested in a live rabbit liver to probe radical-mediated hydroxylation and peroxidation in vivo, respectively, during local irradiation. The levels of serum 8-OHdG in mice were determined (with competitive ELISA) as the biomarker of DNA-related hydroxylation after whole-body irradiation. The levels of liver MDA were measured as the biomarker of lipid peroxidation. The liver ATPase activity of ATP enzymolysis was measured to assess bio-molecular function. All biochemical markers and probes were compared with tissue ^{15}O and ^{11}C activities in live animals.

Supplementary Materials

Acknowledgements

This work was supported by R & D foundation of Top Grade & Kang-Ming Ltd, Beijing China. We gratefully acknowledge the Nanjing Jiancheng Bioengineering Institute (China), Shanghai Hu-Feng Biotechnology Company Ltd. (China) for assistance in the determinations of OH• scavenging capacity, carbonyls, MDA,8-OHdG, hydrated formaldehyde. We are grateful to Dr Li Yun and Jing Yao-hui for their support in conducting the irradiation procedure and to Sha-sha Cao for her assistance in experiments.

Author contributions

J.Z. developed the concept, designed experiments and prepared the manuscript; Q.Y.S and T.S. supervised the project; J.Z., J.H.S., J.H.H., Q.S.Z. performed experiments; W.H.X., C.Y.L., and X.J.C. gave technical support.

Reference List

1, Möckel D, et al. Quantification of beta+ activity generated by hard photons by means of PET. Phys Med Biol. 2007;52(9):2515-30. [PMID: 17440249]

2, Pshenichnov I, et al. PET monitoring of cancer therapy with ^{3}He and ^{12}C beams: a study with the GEANT4 toolkit. Phys Med Biol. 2007;52(24):7295-312. [PMID: 18065840]

3, Fiedler F, et al. On the effectiveness of ion range determination from in-beam PET data. Phys Med Biol. 2010;55(7):1989-98. [PMID: 20224157]

4, Janek S, et al. Development of dose delivery verification by PET imaging of photonuclear reactions following high energy photon therapy. Phys Med Biol. 2006;51(22):5769-83. [PMID: 17068364]

5, Brahme A. Biologically optimized 3-dimensional in vivo predictive assay-based radiation therapy using positron emission tomography-computerized tomography imaging. Acta Oncol. 2003;42(2):123-36. [PMID: 12801131]

6, Carrie J. et al. Francisco. Hydroxyl Radical Substitution in Halogenated Carbonyls: Oxalic Acid Formation. J. Phys. Chem. A, 2010, 114 (8), 2806–2820. [PMID: 20131850]

7, Milosavljevic BH, Laverne JA. Pulse radiolysis of aqueous thiocyanate solution. J Phys Chem A. 2005;109(1):165-8. [PMID: 16839102]

8, Ohshima H, et al. Reactions between hydroxyl-radical-induced 7,8-dihydro-8-oxo-2'-deoxyguanosine precursor and the spin trap alpha-phenyl-N-tert-butylnitrone. J Radiat Res (Tokyo). 1997;38(1):15-25. [PMID: 9164077]

9, Kamada F, et al. Mineralization of aromatic compounds by brown-rot basidiomycetes - mechanisms involved in initial attack on the aromatic ring. Microbiology. 2002;148(Pt 6):1939-46. [PMID: 12055313]

10, Geissler JF, Harwood CS, Gibson J. Purification and properties of benzoate-coenzyme A

ligase, a Rhodopseudomonas palustris enzyme involved in the anaerobic degradation of benzoate. J Bacteriol. 1988;170(4):1709-14. [PMID: 3350788]

11, Kasai H, Nishimura S. Hydroxylation of guanine in nucleosides and DNA at the C-8 position by heated glucose and oxygen radical-forming agents. Environ Health Perspect. 1986;67:111-6. [PMID: 3757945]

12, Xu KY, Zweier JL, Becker LC. Hydroxyl Radical Inhibits Sarcoplasmic Reticulum Ca2+-ATPase Function by Direct Attack on the ATP Binding Site. Circ Res. 1997;80(1):76-81. [PMID: 8978325]

13, Gao J, Yao Y, Squier TC. Oxidatively modified calmodulin binds to the plasma membrane Ca-ATPase in a nonproductive and conformationally disordered complex. Biophys J. 2001;80(4):1791-801. [PMID: 11259292]

14, McCay PB, Reinke LA, Rau JM. Hydroxyl radicals are generated by hepatic microsomes during NADPH oxidation: relationship to ethanol metabolism. Free Radic Res Commun. 1992;15(6):335-46. [PMID: 1314760]

15, Grimsrud PA, et al. Oxidative stress and covalent modification of protein with bioactive aldehydes. J Biol Chem. 2008;283(32):21837-41. [PMID: 18445586]

16, Huang, D. et al. Development and validation of oxygen radical absorbance capacity assay for lipophilic antioxidants using randomly methylated cyclodextrin as the solubility enhancer. J.Agric. Food Chem. 2002, 50, 1815-1821. [PMID: 11902917]

17, Terlouw SA, et al. Metabolite anion carriers mediate the uptake of the anionic drug fluorescein in renal cortical mitochondria. J Pharmacol Exp Ther. 2000;292(3):968-73. [PMID: 10688611]

18, Wallace MB, et al. The safety of intravenous fluorescein for confocal laser endomicroscopy in the gastrointestinal tract. Aliment Pharmacol Ther. 2010;31(5):548-52. [PMID: 20002025]

19, Del Rio D, Stewart AJ, Pellegrini N. A review of recent studies on malondialdehyde as toxic molecule and biological marker of oxidative stress. Nutr Metab Cardiovasc Dis. 2005;15(4):316-28. [PMID: 16054557]

20, Koc M, et al. Melatonin protects rat liver against irradiation-induced oxidative injury. J Radiat Res (Tokyo). 2003;44(3):211-5. [PMID: 14646223]

21, Huang D, Ou B, Prior RL. The chemistry behind antioxidant capacity assays. J Agric Food Chem. 2005;53(6):1841-56. [PMID: 15769103]

22, Reece SY, Hodgkiss JM, Stubbe J, Nocera DG. Proton-coupled electron transfer: the mechanistic underpinning for radical transport and catalysis in biology. Philos Trans R Soc Lond B Biol Sci. 2006;361(1472):1351-64. [PMID: 16873123]

23, Okunieff P, et al. Antioxidants reduce consequences of radiation exposure. Adv Exp Med Biol. 2008;614:165-78. [PMID: 18290327]

24, Gillard N, et al. Radiation-induced oxidative damage to the DNA-binding domain of the lactose repressor. Biochem J. 2007;403(3):463-72. [PMID: 17263689]

25, Maleknia SD, Wong JW, Downard KM. Photochemical and electrophysical production of radicals on millisecond timescales to probe the structure, dynamics and interactions of proteins. Photochem Photobiol Sci. 2004;3(8):741-8.[PMID: 15295629]

26, Gerschman R, et al. Oxygen poisoning and x-irradiation: a mechanism in common. Science 1954;119:623–6. [PubMed: 13156638]

27, Harman D. Aging: A theory based on free radical and radiation chemistry. J Gerontol 1956;11:298–300. [PubMed: 13332224]

28, Harman D. Mutation, Cancer, and Aging. Lancet 1961;1:200–1. [PubMed: 13711615]

28, Wells PG, et al. Oxidative stress in developmental origins of disease: teratogenesis, neurodevelopmental deficits, and cancer. Toxicol Sci. 2009;108(1):4-18. [PMID: 19126598]

30, Berg D, Youdim MB, Riederer P. Redox imbalance. Cell Tissue Res. 2004;318(1):201-13. [PMID: 15365815]

31, Bergamini CM, et al. Oxygen, reactive oxygen species and tissue damage. Curr Pharm Des. 2004;10(14):1611-26. [PMID: 15134560]

32, Freinbichler W, et al. The detection of hydroxyl radicals in vivo. J Inorg Biochem. 2008;102(5-6):1329-33. [PMID: 18262275]

33, Torres-Roca JF, Stevens CW. Predicting response to clinical radiotherapy: past, present, and future directions. Cancer Control. 2008;15(2):151-6. [PMID: 18376382]

34,Ward JF. DNA damage produced by ionizing radiation in mammalian cells: identities, mechanisms of formation, and reparability. Prog Nucleic Acid Res Mol Biol. 1988;35:95-125. [PMID: 3065826]

35, Yamaguchi H, et al. Estimation of yields of OH radicals in water irradiated by ionizing radiation. J Radiat Res (Tokyo). 2005;46(3):333-41. [PMID: 16210790]

Figure 1. Male animals with similar body weight and kept in the same physiological conditions were randomly selected for irradiation studies. Tissue "fingerprints" of photonuclear reactions in live animals are shown for mice (A), rats (B) and rabbits (C). The tissue "fingerprints" of ^{15}O and ^{11}C are unique to each individual.

Figure 2. Tissue "fingerprints" faded away soon after death. Four rabbits were randomly selected for irradiation studies (A-D). The tissue "fingerprints" were unique for each rabbit (A, B) and were also very different between ^{15}O (A) and ^{11}C (B) within each rabbit. Tissue "fingerprints" were lost at 30 min after respiratory and cardiac arrest, i.e., the distributions of ^{15}O (C) and ^{11}C (D) became similar among individuals and similar between ^{15}O (C) and ^{11}C (D) within each individual. An example of dynamic loss of the tissue "fingerprint" is shown in Fig. 2E. The rat tissue "fingerprint" of ^{11}C (E-1) was diminishing at 1 min (E-2), 3 h (E-3), and 18 h (E-4) after respiratory and cardiac arrest. A dynamic decrease of the whole-body $^{15}O/^{11}C$ ratio was recorded after death in SD rats (n=6 at each point), where the * and # represent p-value <0.05 and <0.001, respectively, compared with the live animals (F). As a result of losing tissue "fingerprints", the pattern of $^{15}O/^{11}C$ in organs changed from before (G) and 15 min after (H) the respiratory and cardiac arrest of SD rats (n=6) from heterogeneous to homogeneous, where the * represents p-value<0.05 compared with live animals (n=6).

Figure 3. Using two-phase systems of 1,2-dibromoethane-water (3ml:3ml), water contained ^{16}O and 1,2-dibromoethane had ^{12}C. Radical reactions were initiated by exposing liposomes of 1,2-dibromoethane-water to high-energy beams. The major activity of ^{15}O (A-1) and much smaller activities of ^{11}C and bromine (A-2) were released into the aqueous phase with 0.0163±0.0021μmol/ml of carbonyl products. After subtraction of the contamination of ^{11}C and bromine activities, there was an 8.5-fold increase in the total ^{15}O activity (B, n=12), and the ^{15}O activity from carbonyl products was calculated to be an average of 24,640,994±3,438,904 times that of the water control. As controls, 1,2-dibromoethane and water were irradiated separately so that radical attack (to

1,2-dibromoethane) would not occur. In addition to the background activity of water, ^{15}O (A-4) and ^{11}C (A-5) activities from carbonyl products were not detected in the aqueous phase of the control. After a 3-hr decay of β+ activity, a second irradiation was separately carried out on the aqueous and organic phases of A-1. Radical attack would not be expected, so the result (A-3) was similar to the control. In the live animal studies, benzoic acid was used as the in vivo probe. After 5.5 Gy of local delivery, accumulation of hydroxylated products of benzoic acid has an excellent correlation with the ^{15}O activity (C) but a poor correlation with ^{11}C activity (E) in rabbit livers. After simultaneous exposure to whole-body irradiation, the whole-body ^{15}O activity of mice correlates well with the levels of serum 8-OHdG (D). Whole-body ^{11}C activity is not correlated with levels of serum 8-OHdG (F).

Figure 4. For the ethanol-water mixture (v:v=1:2), radical reactions were initiated by irradiation (A-1 and A-3). As a control, ethanol and water were irradiated separately and were mixed post-irradiation so that the attack (to ethanol) did not occur (A-2 and A-4). There is no difference in the ^{15}O activity between the attack (A-1 and B red column, n=12) and control (A-2 and B black column, n=12) samples. However, ^{11}C activity was significantly higher in the samples with radical attack (A-3 and B red column, n=12) than in the control samples (A-4 and B black column, n=12). Because 0.0109±0.0014 μmol/ml of carbonyl products was detected, the ^{11}C activity from oxidation products was calculated to be an average of 986,961±88,126 times that of the ethanol control. In live animal studies with irradiation with 5.5 Gy of local delivery, the oxidation of FL is well correlated with the ^{11}C activity (C) but poorly correlated with the ^{15}O activity (E) in rabbit liver. After simultaneous exposure to whole-body irradiation, the levels of MDA have a good relationship with ^{11}C activity (D), but they have no correlation with ^{15}O activity (F) in rat liver.

Table1. OH·and/or e_{aq}- attack to methanol at oxygen-free (N_2), oxygenated (O_2), and hydrated electron-free (N_2O/O_2) conditions. For determination of formaldehyde and carbonyls, n=6. For activity counting, n=12.

	Oxygen-free	Oxygenated	Hydrated electron-free
Formaldehyde (μmol/ml)	0.00179±0.00129	0.00195±0.00080	0.00210±0.00115
Carbonyls (μmol/ml)	0.00339±0.00092	0.00381±0.00134	0.00315±0.00128
Formaldehyde: formic acid	1.00:0.89	1.00:0.95	1.00:0.50
^{11}C: ^{15}O	0.11:1.00	0.14:1.00	0.19:1.00
Induced ^{15}O (cpm/μmol)	225779.8±110994.5*	119252.9±60590.2	163716.7±87494.9
Induced ^{11}C (cpm/μmol)	25384.9±10808.9	17224.6±8710.6	30543.0±9712.4**

*At oxygen-free condition, e_{aq}- attack can further increase ^{15}O activity (p=0.01846) compared with oxygenated condition.

** At e_{aq}- free condition, OH·attack can further increase ^{11}C activity (p=0.00470) compared with oxygenated condition.

Figure 1

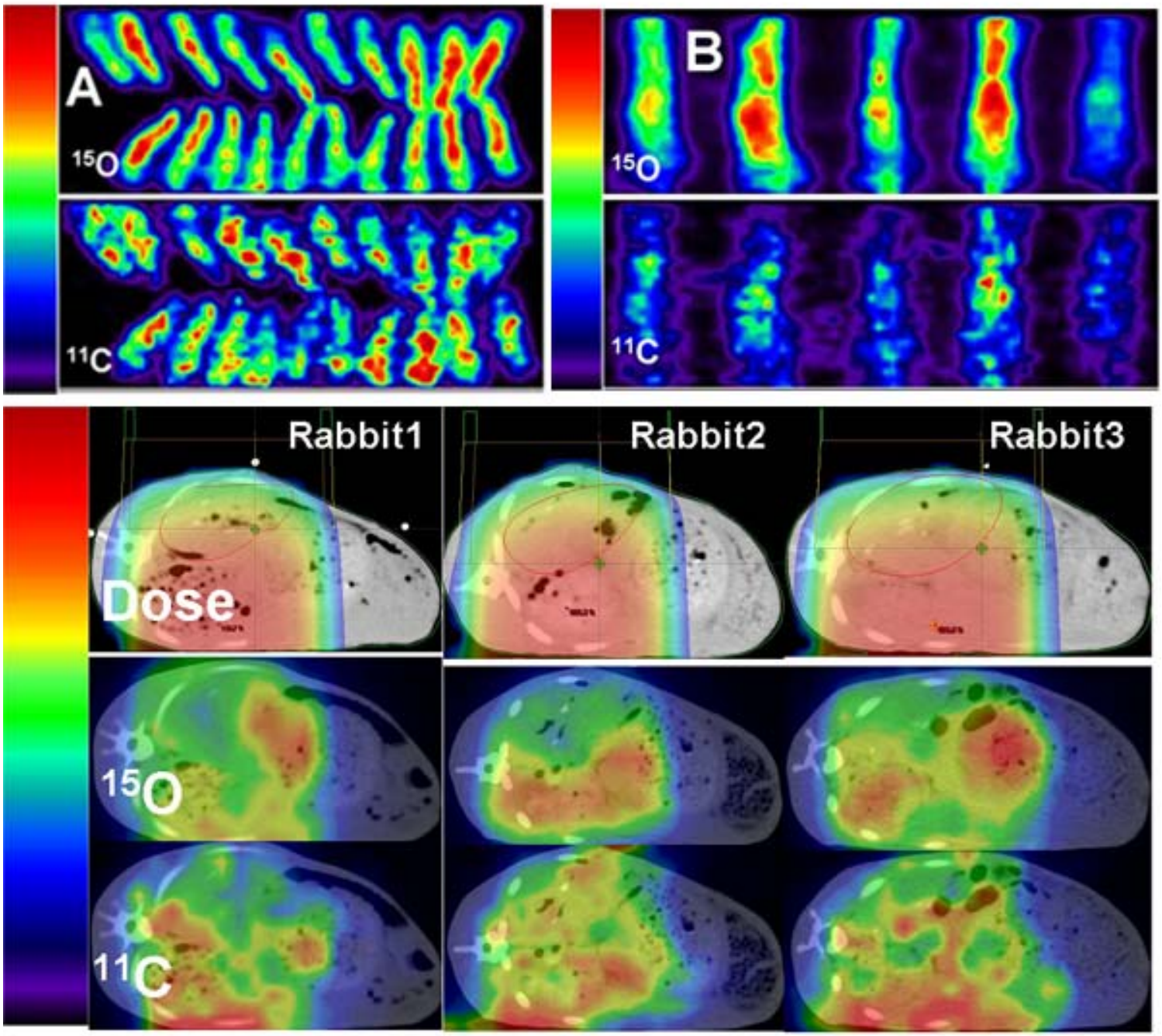

Figure 2

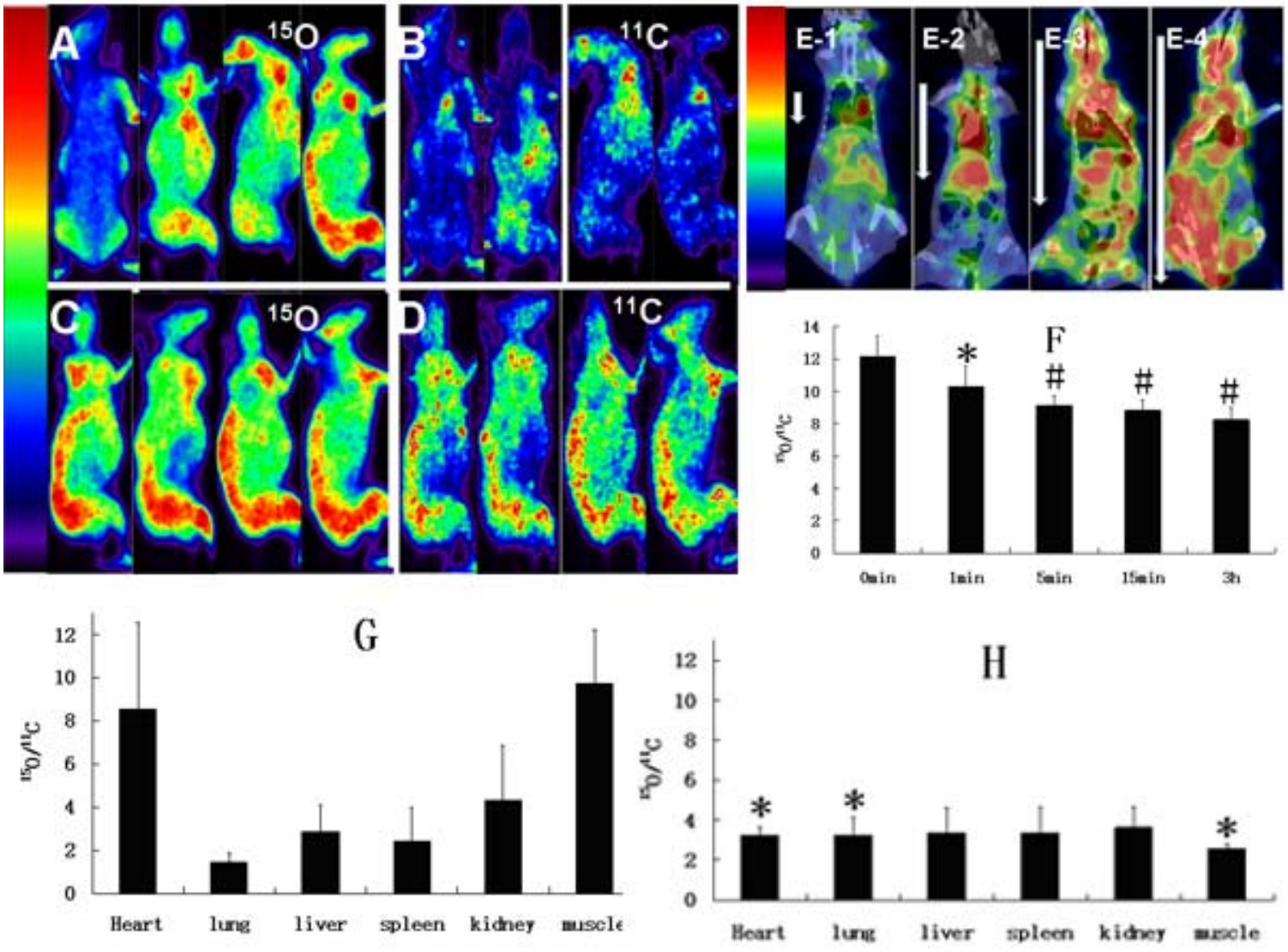
A
15O
B
11C
C
15O
D
11C
E-1
E-2
E-3
E-4
F
*
#
#
#
0min
1min
5min
15min
3h
G
Heart
lung
liver
spleen
kidney
muscle
H
*
*
*
Heart
lung
liver
spleen
kidney
muscle

Figure 3

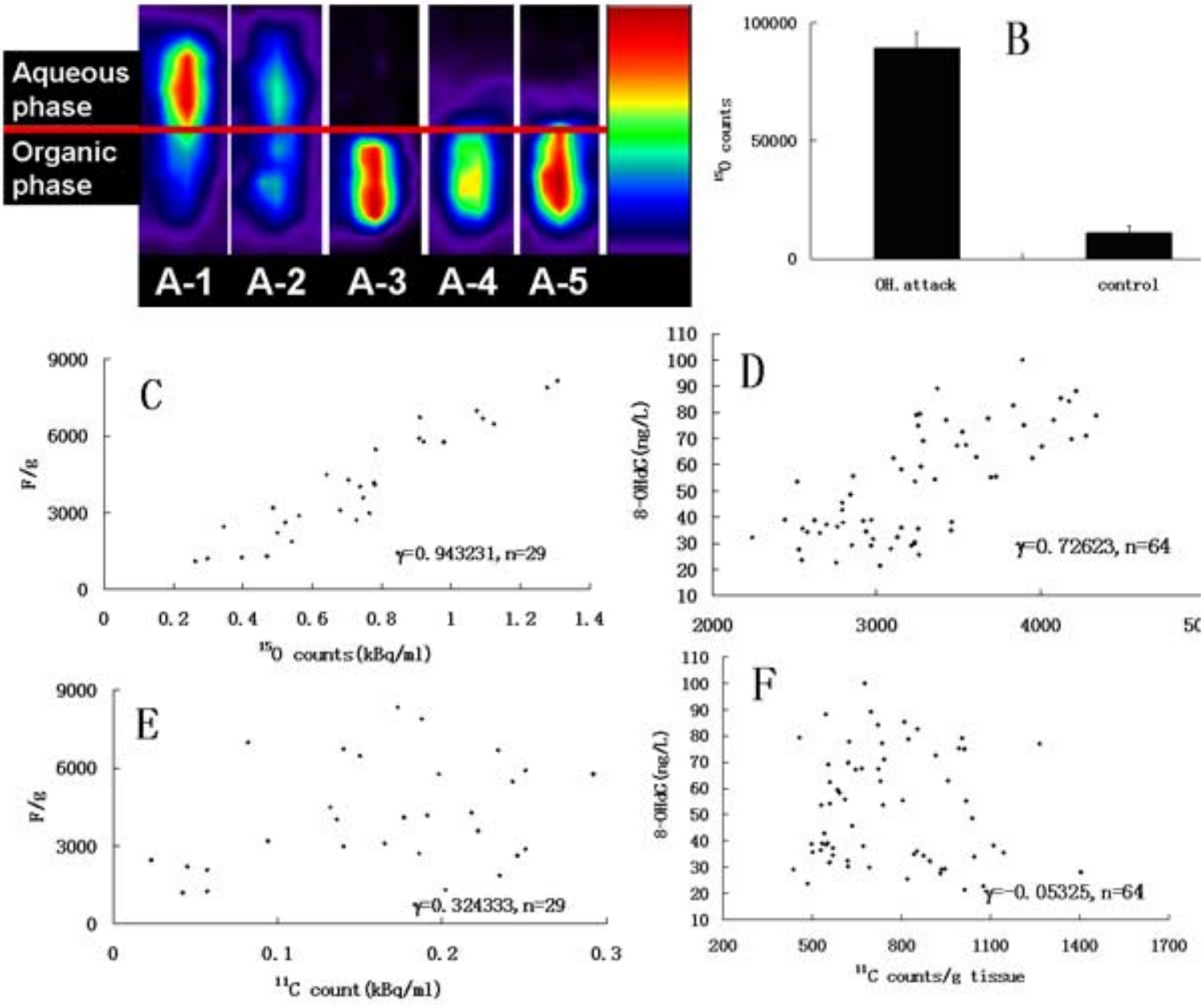
Aqueous phase
Organic phase
A-1
A-2
A-3
A-4
A-5
B
100000
50000
0
OH. attack
control
C
9000
6000
3000
0
F/g
γ=0.943231, n=29
0
0.2
0.4
0.6
0.8
1
1.2
1.4
D
110
100
90
80
70
60
50
40
30
20
10
γ=0.72623, n=64
2000
3000
4000
E
9000
6000
3000
0
F/g
γ=0.324333, n=29
0
0.1
0.2
0.3
F
110
100
90
80
70
60
50
40
30
20
10
γ=-0.05325, n=64
200
500
800
1100
1400
1700
11C counts/g tissue

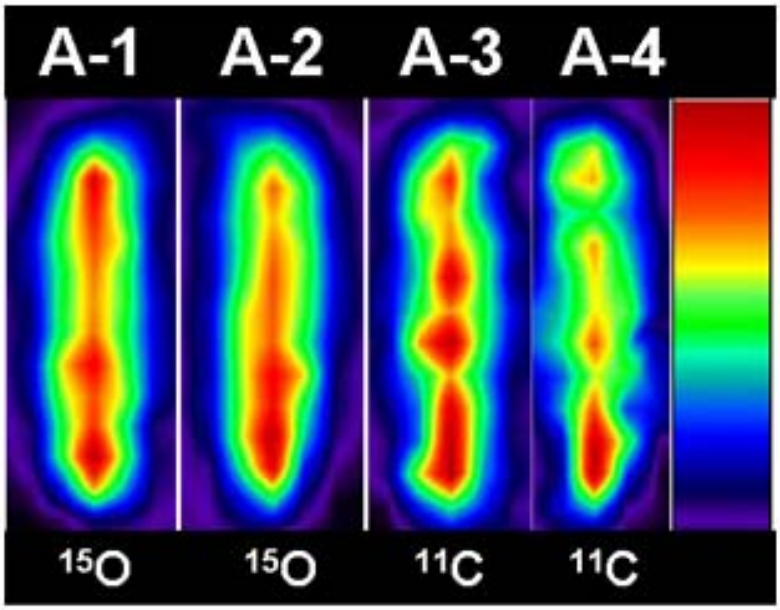
A-1
A-2
A-3
A-4
15O
15O
11C
11C

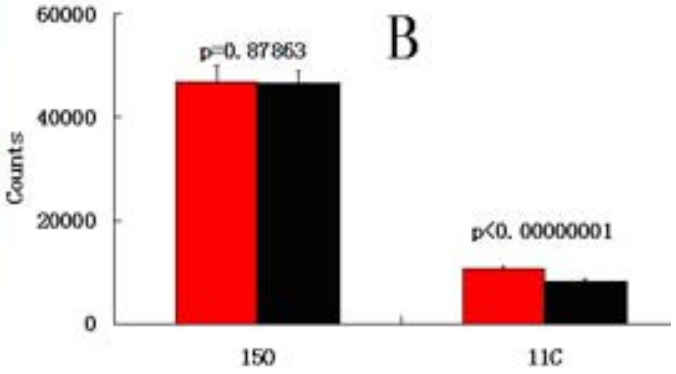
B
60000
40000
20000
0
Counts
p=0.87863
p<0.00000001
15O
11C

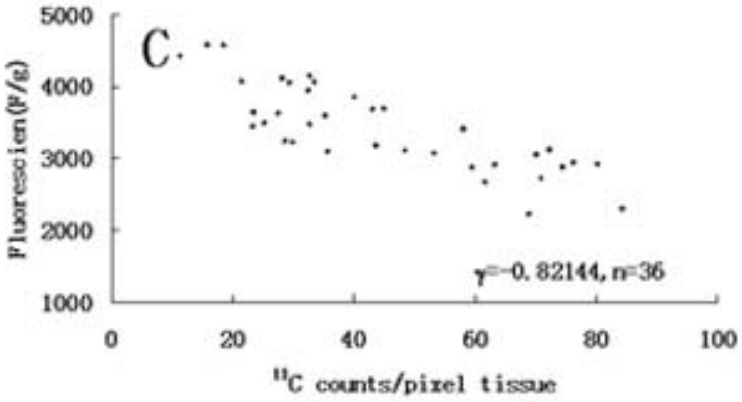
C
5000
4000
3000
2000
1000
Fluorescien(F/g)
γ=-0.82144, n=36
0
20
40
60
80
100
11C counts/pixel tissue

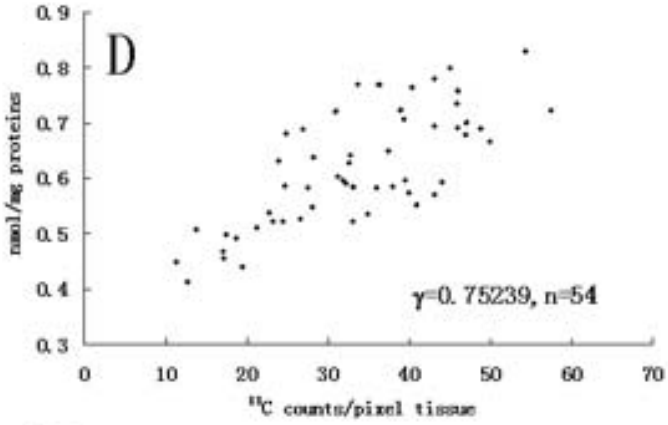
D
0.9
0.8
0.7
0.6
0.5
0.4
0.3
nmol/mg proteins
γ=0.75239, n=54
0
10
20
30
40
50
60
70
11C counts/pixel tissue

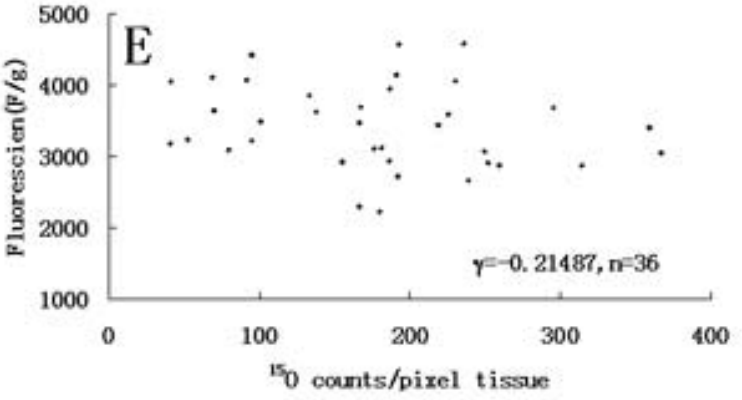
E
5000
4000
3000
2000
1000
Fluorescien(F/g)
γ=-0.21487, n=36
0
100
200
300
400
15O counts/pixel tissue

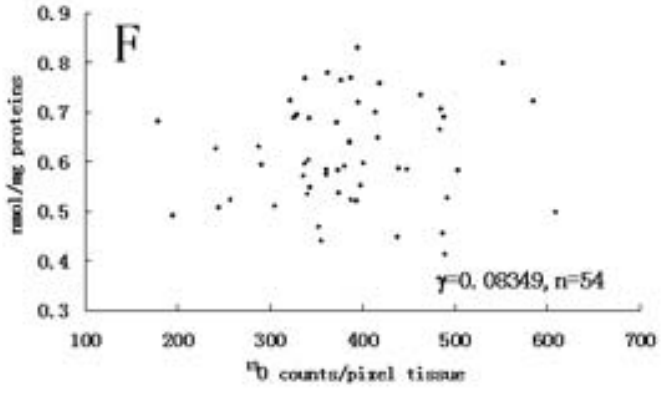
F
0.9
0.8
0.7
0.6
0.5
0.4
0.3
nmol/mg proteins
γ=0.08349, n=54
100
200
300
400
500
600
700
15O counts/pixel tissue